Chemical ozone loss in the Arctic winter 1991–1992

S. Tilmes, R. Müller, R. J. Salawitch, U. Schmidt, C. R. Webster, H. Oelhaf, J. M. Russell Iii, C. C. Camy-Peyret

Atmos. Chem. Phys. Discuss., 7, 10097–10129, 2007
www.atmos-chem-phys-discuss.net/7/10097/2007/

Atmospheric Chemistry and Physics Discussions

Chemical ozone loss in the Arctic winter 1991–1992

S. Tilmes[1], R. Müller[2], R. J. Salawitch[3], U. Schmidt[4], C. R. Webster[3], H. Oelhaf[5], J. M. Russell III[6], and C. C. Camy-Peyret[7]

[1]National Center for Atmospheric Research, Boulder, Colorado, USA
[2]Institute of Stratospheric Research (ICG-I), Forschungszentrum Jülich, Germany
[3]Jet Propulsion Laboratory, California Institute of Technology, California, USA
[4]J.W. Goethe University Frankfurt, Germany
[5]IMK-ASF, Forschungszentrum Karlsruhe, Karlsruhe, Germany
[6]Hampton University, Virginia 23668, USA
[7]Universite Pierre et Marie Curie and CNRS, Ivry-sur-Seine, France

Received: 20 April 2007 – Accepted: 4 July 2007 – Published: 12 July 2007

Correspondence to: S. Tilmes (tilmes@ucar.edu)

Abstract

Chemical ozone loss in winter 1991–1992 is recalculated based on observations of the HALOE satellite instrument, ER-2 aircraft measurements and balloon data. HALOE satellite observations are shown to be reliable in the lower stratosphere below 400 K, at altitudes where profiles are most likely disturbed by the enhanced sulfate aerosols, as a result of the Mt. Pinatubo eruption in June 1991. Very large chemical ozone loss was observed below 400 K from Kiruna balloon observations between December and March 1992. Additionally, for the two winters after the Mt. Pinatubo eruption, HALOE satellite observations show a stronger extent of chemical ozone loss at lower altitudes compared to other Arctic winter between 1991 and 2003. In stipe of already occurring deactivation of chlorine in March 1992, Mipas-B and LPMA balloon observations indicate still chlorine activation at lower altitudes, consistent with observed chemical ozone loss occurring between February and March and April. Enhanced chemical ozone loss in the Arctic winter 1991–1992 as calculated in earlier studies is corroborated here.

1 Introduction

The Arctic winter 1991–1992 was a climatological moderately warm winter. For this winter, chemical processes in the polar vortex were strongly influenced by the enhanced burden of sulfate aerosols after the eruption of Mt. Pinatubo in June 1991. Strong chlorine activation and significant chemical ozone loss was observed (e.g., Waters et al., 1993; Toohey et al., 1993; Proffitt et al., 1993; Salawitch et al., 1993; Brandtjen et al., 1994). The amount of chemical ozone loss was quantified in several previous studies (e.g., Proffitt et al., 1993; Rex et al., 1998; Müller et al., 2001). These studies were based on different data sets: ER-2 aircraft measurements from the Airborne Arctic Stratospheric Expedition II (AASE-II) (Anderson et al., 1991; Toohey et al., 1993), data from the European Arctic Stratospheric Ozone Experiment (EASOE) (Pyle et al., 1994), namely observations from balloon-borne whole air samplers and ozone sondes.

ACPD

7, 10097–10129, 2007

Further ozone loss was derived using satellite observations from the Halogen Occultation Experiment (HALOE) aboard the UARS satellite (Russell et al., 1993) and from the UARS microwave limb sounder (MLS) measurements (Tilmes et al., 2004; Manney et al., 2003)

These studies consistently found ozone loss of ≈25% in mid-winter (up to the end of January) and large ozone loss rates during January (Salawitch et al., 1993; von der Gathen et al., 1995). Further, model studies for January indicated largest chemical ozone loss in the outer part of the vortex due to a longer solar exposure (Lefèvre et al., 1994). Müller et al. (2001) and Tilmes et al. (2004) derived chemical ozone loss from HALOE satellite observations between 72 and 90 DU in February, March and April, using tracer-tracer correlations. Largest loss in column ozone was found below 450 K. However, especially below 400 K the burden of aerosol particles in this year was strongly enhanced due to the volcanic eruption of Mt Pinatubo in June 1991. Retrieved HALOE O_3 mixing ratios were strongly overestimated in situations of heavy aerosol loading before a correction had been applied. After a correction of the data, the uncertainty of O_3 mixing ratios in the peak aerosol layer is 25% (Hervig et al., 1995).

It is well established that enhanced stratospheric sulphate aerosol leads to greater halogen induced chemical ozone destruction (e.g., Cox et al., 1994; Tabazadeh et al., 2002; Rex et al., 2004; Tilmes et al., 2004; WMO, 2007). Model simulations by Tabazadeh et al. (2002) predicted a large increase of chemical ozone loss values after a strong volcanic eruption, especially at lower altitudes (below 17 km). For the Arctic winters 1991–1992 and 1992–1993, after the eruption of Mt. Pinatubo, Tilmes et al. (2006) reported strong chemical ozone loss based on an analysis of HALOE satellite observations. These values are outliers from the compact empirical relationship between chemical ozone loss and the PSC (polar stratospheric cloud) formation potential (PFP)[1] for winters between 1991 and 2005, as shown in Fig. 1. Winter 1991/92 was characterized by a relatively small PFP value that indicates a climatologically warm win-

[1] PFP presents the fraction of the vortex, over an ozone loss season in Arctic or Antarctica, exposed to PSC temperatures (Tilmes et al., 2006).

ACPD
7, 10097–10129, 2007

ter. Based on this relationship, the influence of enhanced sulfate aerosols on chemical ozone loss is about 40 DU for altitudes between 380–550 K potential temperature and about 20 DU between 400–500 K potential temperature in winter 1991–1992 (Tilmes et al., 2006). However, up to now it is not proved that the enhanced chemical ozone loss derived in that study is a result of chemical processes, or if observations are wrongly effected by the enhanced sulfate aerosols. Rex et al. (2004) reported the impact of enhanced sulphate aerosol on chemical ozone loss to be smaller based on ozone sonde data than in Tilmes et al. (2006) (about 10 DU between 400–550 K) for this winter. For winter 1992–1993, Rex et al. (2006) do not find a significant impact of enhanced sulphate aerosol on ozone loss.

As described above, the presence of the sulphate aerosol in the stratosphere caused by the eruption of Mt. Pinatubo has also severely affected the remote sensing measurements of the radiometer channels of the HALOE experiment (Hervig et al., 1995). Here, we will address the question whether the large chemical ozone loss values during spring 1992 based on HALOE observations (Tilmes et al., 2006) are an artifact caused by uncertain observations, or if this much ozone loss can result from chemical processes not included in the PFP value used for the linear relationship in Fig. 1.

The goal of this paper is to derive a reliable value of chemical ozone loss for the winter 1991–1992. For the first time for this winter, we combine all relevant available in-situ observation, which are balloon-borne tracer measurements (Schmidt et al., 1994; Müller et al., 2001) and high-altitude aircraft ER-2 measurements (Proffitt et al., 1993) to validate the HALOE satellite observations. We will show that HALOE observations in winter 1991–1992 are reliable, especially at lower altitudes. This finding should be also conferable for measurements in winter 1992–1993, a winter that also shows a strongly enhanced aerosol burden. In this way, the impact of sulfate aerosols on chemical ozone loss can be further discussed elsewhere.

Tracer-tracer correlations are used to derive chemical ozone loss as described in Sect. 2. Using this technique transport processes within the polar vortex are accounted for. Compared to other methods, this has the advantage that a possible mis-calculation

ACPD
7, 10097–10129, 2007

of transport processes from models for a winter shortly after the volcanic eruption (Robock, 2001) do not affect the calculation of chemical ozone loss. We consider various observations, as there are aircraft, balloon and satellite observations to describe the reliability of the data sets, as described in Sect. 3. The meteorology of the Arctic winter 1991–1992 is described in Sect. 4. Depending on the location of the observations, either inside or further outside the polar vortex, air masses indicate different characteristics. The location of measurements with respect to the polar vortex will be discussed in detail in Sect. 5. Based on this information, chemical ozone loss is derived as described in Sect. 6. Further, a comparison of ozone loss profiles for different Arctic winters will be discussed.

Chemical ozone loss is a result of chlorine activation in connection with sunlight in the polar vortex. Starting in late December 1991, strong chlorine activation and enhanced ClO were observed until late February in the Arctic lower stratosphere (Waters et al., 1993; Toohey et al., 1993). Enhanced OClO is reported for as late as 11 March (Brandtjen et al., 1994). In Sect. 7, we use balloon measurements in mid-March 1992 (von Clarmann et al., 1993; Oelhaf et al., 1994; Wetzel et al., 1995) to further scrutinize the vertical structure of chlorine activation in March 1992 in the polar vortex.

2 Method

In this study, the tracer-tracer correlation method is used to derive chemical ozone loss in the Arctic polar vortex. The relationship between ozone and a long-lived tracer will not change in absence of heterogeneous chemistry to cause chlorine activation, because of a sufficiently long life-time of the tracers. Further, if the polar vortex is isolated and mixing across the vortex edge can be neglected, changes from the relation between ozone and a long-lived tracer in the early winter (the early winter reference function) can be assumed to be a result of chlorine activation (e.g. Proffitt et al., 1993; Tilmes et al., 2004).

The validity of the tracer-tracer correlations (TRAC) technique as a method to deduce

ACPD
7, 10097–10129, 2007

chemical ozone loss has been debated in the literature (e.g., Michelsen et al., 1998; Plumb et al., 2000; Salawitch et al., 2002; Tilmes et al., 2004; Müller et al., 2005, and references therein). Plumb et al. (2000) state that "estimates of ozone depletion inferred from O_3: tracer relations are likely to be overestimates" due to effect of mixing across the vortex edge. As summarized in the following, this concern is not valid under the conditions considered here. In the conceptual model used by Plumb et al. (2000) diffusivities for transport across the vortex edge are employed that are very likely too high by more than an order of magnitude (Müller et al., 2005). Moreover, the conceptual model is formulated in terms of artificial, chemically inert tracers χ_1 and χ_2. Salawitch et al. (2002) have demonstrated that the model results for χ_1 and χ_2 should not be applied to the interpretation of the O_3/N_2O relation in the Arctic vortex. In the model used by Plumb et al. (2000), the development of the χ_1-χ_2 relation is driven primarily by supply of air at the top of the vortex with near zero mixing ratios of both species. However, ozone mixing ratios at the top of the vortex are typically greater than those in the vortex after chemical ozone loss occured. Even though air low in ozone exists in the mesosphere, photochemical model calculations indicate that O_3 is quickly regenerated to mixing ratios of 3–4 ppm by normal gas phase photochemistry as these air parcels descend to lower than ≈40 km (Salawitch et al., 2002). Indeed ozone mixing ratios ranging between 3.6–5.6 ppm have been measured in the mesospheric air-masses that have intruded into the Arctic stratosphere in early 2003 (Müller et al., 2007[2]).

To apply the technique carefully (Tilmes et al., 2004; Müller et al., 2005), the location of profiles have to be discussed with respect to the polar vortex edge to understand if they are influenced by air masses from outside the vortex. Profiles which are located within or outside the boundary region of the polar vortex show different characteristics. A detailed description of the technique and a discussion of the uncertainties due to mixing processes is given in Tilmes et al. (2004) and Müller et al. (2005). The polar

[2]Müller, R., Tilmes, S., Grooß, J.-U., Engel, A., Oelhalf, H., Wetzel, G., Huret, N., Pirre, M., Catoire, V., Toon, G., and Nakajima, H.: Impact of mesopheric intrusions on ozone-tracer relations in the stratospheric polar vortex, J. Geophys. Res., submitted, 2007.

vortex edge and the poleward edge of the vortex (vortex core) are calculated as defined by Nash et al. (1996), based on the PV gradient as a function of equivalent latitude. A more precise selection of vortex profiles is performed for aircraft observations with a large horizontal resolution, described in Sect. 5. The area of the vortex outside the vortex core is defined as the vortex boundary region.

3 Observations

In this study, we use satellite observations taken from the HALOE instrument (Russell et al., 1993). HALOE measured during January, February, March and April 1992 were within the polar vortex core (vortex boundary region for January). HALOE CH_4 and HF are suitable long-lived tracers to apply to the tracer-tracer correlation method as described in Tilmes et al. (2004). The satellite instrument uses gas filter channels to measure these long-lived tracers, different than ozone, which is observed using radiometer channels. The gas filter channels are only weakly affected by aerosol particles and, therefore, a correction of these species was not necessary (Hervig et al., 1995). Ozone mixing ratios have an uncertainty of 25% in the peak aerosol layer (caused by the Mt. Pinatubo eruption) after a correction of the data (Hervig et al., 1995). Additionally, HCl/tracer relations were investigated in Tilmes et al. (2004) to estimate possible chlorine activation in the polar vortex.

Balloons were launched in Kiruna, Sweden, during the Arctic winter between December 1991 and March 1992 employing cryogenic (Schmidt et al., 1987) and whole air grab sampling techniques (Bauer et al., 1994). Ozone observations were taken by standard electrochemical-concentration-cell sondes (Pyle et al., 1994) and N_2O abundance were measured with balloon-borne whole-air samplers (Bauer et al., 1994). Further for this study, we use ER-2 aircraft observations of N_2O and CH_4 taken by the ALIAS instrument (Webster et al., 1994) and the ATLAS instrument (Loewenstein et al., 1993) and O_3 from the dual beam photometer (Proffitt and McLaughlin, 1983). During January and February, the ER-2 observed well within the polar vortex core. In-situ

ACPD
7, 10097–10129, 2007

balloon and ER-2 observations of ozone mixing ratios are not influenced by enhanced sulfate aerosols in the lower stratosphere and can be used as a comparison to HALOE satellite observations.

We compare O_3 and CH_4 profiles for the different measurements as well as the relationship between O_3/CH_4. N_2O balloon and aircraft observations were converted to CH_4 mixing ratios using a CH_4/N_2O tracer relation derived using whole air sampler measurements, reported in Tilmes et al. (2006).

Additionally, two balloon-borne experiments were launched from Kiruna on 14 March 1992; MIPAS-B took measurements of several trace gases including CH_4 and $ClONO_2$ and LPMA measured HCl and CH_4 (von Clarmann et al., 1993; Camy-Peyret, 1994; Oelhaf et al., 1994; Wetzel et al., 1995). MIPAS-B is a cryogenic Fourier Transform Spectrometer recording limb emission spectra and LPMA performs solar occultation infrared measurements.

4 Meteorology of the Arctic vortex 1991–1992

The polar vortex in winter 1991–1992 was cold between November and January and disturbed by several warming pulses (Naujokat et al., 1992). Temperatures were below 195 K (favorable conditions for chlorine activation by PSCs) only during January (Newman et al., 1993; Manney et al., 2003). Owing to the enhanced sulfate aerosol densities in the lower stratosphere, the potential of chlorine activation also exists during the first part of February and the first half of March 1992 below 450 K. At the end of January, a major warming resulted in weaker, westerly zonal winds at 60° N (Naujokat et al., 1992). Transport of air into the vortex was reported by Grooß and Müller (2003). During February and March, the vortex was stable and broke down during April.

ACPD
7, 10097–10129, 2007

5 Location of the observations

The characteristic of the distribution of long-lived tracers in the polar region strongly depends on the location of observations. In the polar vortex, air masses descend most significantly at the beginning of the winter. Descent results in larger ozone and lower CH_4 mixing ratios within the polar vortex than outside the vortex. Additionally, chemical ozone loss occurs during winter and spring within the Arctic vortex, if vortex temperatures reach values to allow halogen activation, resulting in a decrease of ozone mixing ratios. In the vortex boundary region airmasses are influenced by air from outside the vortex as a result of isentropic mixing and show different distributions compared to airmasses within the polar vortex core. In order to discuss the reliability of satellite data, it is important to compare similar airmasses. We therefore define the location of various observations, based on whether they were observed within the vortex core, in the vortex boundary region or outside the vortex. In Fig. 2, we compare CH_4 and O_3 profiles of available observations in winter 1991–1992.

For HALOE satellite observations, we use the Nash et al. (1996) criterium to distinguish observations that are taken within the polar vortex core, the vortex boundary region and outside the vortex. In the following, only satellite profiles in the vortex and the vortex boundary region (denoted as "entire vortex") are considered. For ER-2 observations, only the part of the flight path within the entire polar vortex is considered. We use the potential vorticity P from NMC, interpolated on the flight path to distinguish between measurements that have being taken inside and outside the polar vortex, as described in the following. The modified potential vorticity (Lait, 1994; Müller and Günther, 2003) $\Pi = P \cdot (\theta_0/\theta)^{-\varepsilon}$ is employed, where θ is the potential temperature, θ_0=475 K is a reference potential temperature and the exponent ε may be chosen to adjust the scaling to the prevailing temperature profile (Müller and Günther, 2003). Here, we use ε=4.5, based on the approximately isothermal temperature profiles measured by radiosonde and by the Microwave Temperature Profiler (MTP) aboard the ER-2 in January/February 1992. The modified potential vorticity Π is scaled to θ_0=475 K.

ACPD
7, 10097–10129, 2007

The potential vorticity at the edge of the vortex is calculated to be P=29 PVU (potential vorticity units) and at the vortex core to be P=34 PVU during January and February 1992, using MetO data based on the Nash et al. (1996) criterion. Measurements with Π larger 29 PVU are denoted to the entire vortex (dotted lines) and measurements with Π larger than 34 PVU are denoted to the vortex core (solid lines in Fig. 2).

Some of the available Kiruna balloon profiles represent the airmass composition at various locations relative to the vortex boundary as described by Bauer et al. (1994) and Schmidt et al. (1994) and discussed below.

In Fig. 2, CH_4 and O_3 mixing ratios are shown for different periods and different observations. In each panel, a to f, two Kiruna balloon data are shown as black and red dashed lines. The profile taken on 5 December 1991, black line, was located well inside the vortex for all altitudes. The profile taken on 12 December 1991, red line, was partly located inside the polar vortex, for altitudes above 475 K, and partly outside but close to the vortex edge for altitudes at and below 475 K (compare Fig. 3, top row). Kiruna observations within the entire vortex are used as a reference for early winter conditions observed during December.

Figure 2, panels a and b, show ER-2, Kiruna and HALOE observations during January 1992 compared to the two Kiruna balloon observations in December. The Kiruna balloon observations on 18 January are located well inside the vortex, see also Fig. 3, middle, left panel.

Smaller CH_4 mixing ratios compared to the reference profiles is a result of descent of the polar vortex between December and January. Profiles taken on 22 and 31 January 1992, over Kiruna, are located outside the polar vortex at altitudes below 500 K (see Fig. 3, bottom panels). Above 500 K, the measurements show vortex characteristics with smaller CH_4 mixing ratios compared to the reference profiles. The flight direction of the balloon, especially for the 31st of January, has possibly moved toward the vortex core. Additionally, ER-2 aircraft observations were taken at locations between outside the vortex and deep inside the polar vortex on 20 January (Fig. 3, middle right panel, white triangles). Observations taken in the boundary area of the vortex show larger

CH_4 mixing ratios (dotted lines in Fig. 2, panel a). ER-2 CH_4 mixing ratios and their deviation from the reference in the vortex core are in good agreement with the balloon observations over Kiruna on 18 January 1992. One HALOE satellite profile, taken on 14 January within the vortex boundary region (panel a and b, cyan diamonds), does not show lower CH_4 mixing ratios and was possibly influenced by air from outside the vortex.

The corresponding O_3 profiles observed in January 1992 indicated minor deviations from the reference profile (see Fig. 2, panel b). ER-2 ozone mixing ratios and the balloon profile on January 18, observed within the vortex core, are slightly larger compared to the reference function due to the descent of vortex air masses. Kiruna balloon data on January 22 and 31 and HALOE observations in January show smaller ozone mixing ratios below 500 K. These profiles were possibly influenced by air masses with smaller ozone mixing ratios from outside the vortex, as also explained by Müller et al. (2001). The smaller ozone mixing ratios on 18 January above 550 K might be the result of the influence of outer vortex air.

In Fig. 2 panel c to f, we compare CH_4 and O_3 mixing ratios of HALOE satellite observations taken within the vortex with Kiruna balloon observations (panel c and d) and ER-2 observations (panel e and f) during February to April 1992. All HALOE observations show smaller CH_4 mixing ratios compared to the reference profile (panel c and e) and therefore indicate the descent of airmasses within the polar vortex between December and March/April. One HALOE profile was partly observed within the vortex core (below 500 K) on February 8 and several profiles were observed at the end of March and the beginning of April in the polar vortex, as shown in Fig. 4.

Only the Kiruna balloon profile observed in 12 March 1992 (Fig. 2, panel c, green squares) indicates a similar characteristic as the HALOE observations between March and April between 350 and 420 K, at 475 K and above 550 K. During its flight, the balloon moved towards the edge of the vortex for the other altitudes as described by Bauer et al. (1994) and Schmidt et al. (1994). The balloon profile taken over Kiruna on 5 March was located in the vortex boundary region (Fig. 2, panel c, blue squares) and

does not show significant deviations from the reference profiles. Ozone mixing ratios of balloon and satellite observations are in agreement, see panel d.

ER-2 observations are only available within the polar vortex during January and February. All ER-2 observations during March were obtained outside the polar vortex (see Fig. 4). As for January, February observations were taken at locations between the outer vortex and the vortex core. Profiles showing smallest CH_4 mixing ratios and largest O_3 mixing ratios at a certain theta levels were taken deep inside the vortex core. CH_4 profiles taken within the vortex core are in good agreement with HALOE observations. ER-2 ozone mixing ratios (Fig. 2 panel f) are slightly larger in February compared to HALOE observations in March and April for the same potential temperature level. This is in agreement with possible chemical ozone loss that has taken place between February and March/April.

In summary, CH_4 and O_3 mixing ratios of the considered observations agree well if observed within the polar vortex core. Profiles observed outside the polar vortex core show larger CH_4 mixing ratios and smaller O_3 mixing ratios as a result of the influence of outer vortex air. It is shown that HALOE O_3 and CH_4 observations are reliable between 350 and 700 K. Observations are in good agreement with ER-2 observations below 550 K potential temperature and with Kiruna balloon observations taken within the polar vortex core in January and March.

6 Chemical ozone loss

6.1 Tracer-tracer correlations

To estimate chemical ozone loss, we derived a O_3/CH_4 early winter reference function based on balloon observations taken on 5 and 12 December 1991, that are located in the entire polar vortex (Fig. 5, top panel). On 12 December, balloon data were measured well inside the polar vortex core (green symbols). On 5 December only profiles above 475 K were located within the entire vortex (red squares) (Fig. 5, top

ACPD
7, 10097–10129, 2007

panel).

This relation is slightly improved compared to Tilmes et al. (2004) and Müller et al. (2001).

$$O_3 = -12.5 \cdot (CH_4)^5 + 69.2 \cdot (CH_4)^4 - 141.5 \cdot (CH_4)^3 + 128.7 \cdot (CH_4)^2 - 51.3 \cdot CH_4 + 11.1 \quad (1)$$

The standard deviation of the derived reference function is σ=0.29 ppmv. This value is used to calculate the uncertainty of the loss in column ozone.

During January, ER-2 aircraft observations indicate significant deviation from the early winter reference function, (Fig. 5, middle panel). Kiruna balloon observations taken within the vortex core on January 18, as discussed above, agree well with ER-2 observations. Kiruna profiles that are influenced by outer vortex air scatter above the reference function. HALOE observations in January show less deviation from the reference function than ER-2 observations due to the location outside the polar vortex core.

During February, ER-2 observations indicate a larger deviation from the early winter reference function compared to January. Therefore, further chemical ozone loss has occurred. Later in March and April, ER-2 aircraft observations are not considered, because they were taken far outside of the polar vortex (see Fig. 4). HALOE satellite observations during February are in agreement with ER-2 data (Fig. 5 green diamonds and lines). Further, Kiruna balloon data on 12 March show similar deviations from the early winter reference function as HALOE observations obtained in March and April, within the polar vortex core between 350 and 420 K, at 475 K, and above 550 K (as discussed above).

6.2 Local chemical ozone loss

Accumulated ozone loss profiles between December 1991 and observations in January to April 1992 are shown in Fig. 6. During January, local chemical ozone loss up to 1.3 ppmv is reached between 400 K and 480 K based on ER-2 data and Kiruna

ACPD
7, 10097–10129, 2007

balloon data (red squares). In the vortex boundary region, one HALOE profile shows less ozone loss (up to 0.8 ppmv) in January. The observed chemical ozone loss during January is in agreement with the large ozone loss values observed in mid-winter (e.g. von der Gathen et al., 1995). Further, HCl/CH_4 profiles observed by HALOE in the vortex boundary region indicate significant chlorine activation (Tilmes et al., 2004) and strongly enhanced ClO mixing ratios (Waters et al., 1993; Toohey et al., 1993). Between January and February a significant increase of local ozone loss is obvious only for one HALOE profile measured within the polar vortex core. Later in March and April, HALOE observations show local ozone loss values between 1.6 and 2.1 ppmv between 420 and 460 K. Additional ozone loss is possible during March and April due to possible chlorine activation during March, as described in Sect. 7, and the increase in solar illumination on the polar vortex later in spring. Local ozone loss derived using the Kiruna balloon profile on 12 March 1992, (green squares) is in agreement with HALOE observations below 400 K and above 470 K, at altitudes where the balloon was located within the polar vortex core, as discussed above. Further, Kiruna balloon observations during March show large local ozone loss values below 380 K.

The impact of enhanced sulfate aerosols in the lower stratosphere after the Mt. Pinatubo eruption is obvious in comparing averaged ozone loss profiles for March/April of different winters between 1991 and 2003 (see Fig. 7). The winter 1991–1992 and 1992–1993 show enhanced ozone loss at altitudes below 400 K, black and red line, respectively. Further, the maximum ozone loss in winter 1991–1992 is located about 10 K below the maximum of the winter 1992/93 and 1999/2000.

6.3 Chemical loss in column ozone

Chemical ozone loss in winter 1991–1992 is summarized in Figure 8. All derived ozone loss values have an uncertainty of up to 20 DU, due to the uncertainty of the early winter reference function used (see Figure 5, black dotted lines). Between 400–500 K, chemical ozone loss increases from 41 DU in January (observed by ER-2 within the entire vortex) towards 65 DU in April (observed by HALOE), as shown in Fig. 8, green

ACPD
7, 10097–10129, 2007

columns. Between 380 and 550 K, ozone loss reached 74 DU in March and 88 DU in April (blue columns). As discussed above, Kiruna profiles are partly located outside the polar vortex core and show less chemical ozone loss, especially between 400 and 500 K. Nevertheless, balloon data indicate significant chemical ozone loss between January and March below 400 K in agreement with HALOE observations in April.

7 Chlorine activation deduced from MIPAS-B and LPMA measurements

Chemical ozone loss during February and March in the lower polar stratosphere is only possible if chlorine is still activated. Information about the two major chlorine reservoir species, $ClONO_2$ and HCl, is available from the balloon-borne measurements MIPAS-B and LPMA on 14 March 1992. By that time, chlorine deactivation in the Arctic vortex had proceeded where the majority of the active chlorine, $ClO_x(Cl + ClO + 2 \times Cl_2O_2)$, had been converted to $ClONO_2$ (e.g., Toohey et al., 1993; Müller et al., 1994).

The observed sum of HCl and $ClONO_2$, Cl_y, can be calculated from the balloon-borne measurements, to estimate the abundance of inorganic chlorine Cl_y in March 1992. We derived the Cl_y/CH_4 relationship, using the concurrently measured methane mixing ratios and compared it to the Cl_y/CH_4 relation reported by Grooß et al. (2002) for deactivated conditions. Cl_y has been reduced by 12% to account for the lower chlorine loading in 1992 than in 2000 (WMO, 2007). The increase in methane (≈2%) from 1992 to 2000 (Simpson et al., 2002) has only a minor effect but is also taken into account (Fig. 9). The maximum Cl_y of about 3 ppb at the lowest CH_4 mixing ratios is in very good agreement with Cl_y deduced independently from whole air sampler measurements for winter 1991–1992 (Schmidt et al., 1994). Clearly, for methane mixing ratios greater than ≈0.8 ppm the sum of $ClONO_2$ and HCl is much lower than the estimated Cl_y. This indicates that chlorine is not yet completely deactivated at this time.

In Fig.10, the sum of the measured $ClONO_2$ and HCl mixing ratios is compared against the estimated inorganic chlorine Cl_y on a potential temperature scale. Between about 345 and 400 K, Cl_y exceeds the sum of $ClONO_2$ and HCl, showing that

ACPD
7, 10097–10129, 2007

at those altitudes chlorine was still activated. The vertical profiles of HCl and $ClONO_2$ on 14 March 1992 (dashed and dotted lines, respectively in Fig. 10) confirms that the deactivation that has occurred up to this date is dominated by the formation of $ClONO_2$ (e.g., Toohey et al., 1993; Müller et al., 1994). HALOE HCl/CH_4 relations support this finding (Tilmes et al., 2004).

Figure 11 shows the vertical profile of active chlorine on 14 March found as the difference between the estimated Cl_y for deactivated conditions and the observed Cl_y (the sum of the measured $ClONO_2$ and HCl mixing ratios) on 14 March 1992. Maximum active chlorine of ≈1 ppb occurred around 380 K, which could lead to rapid ozone loss due to the long period of sunlight present in March.

8 Discussion

The comparison of different observations in the winter 1991–1992 results in a consistent picture of chemical ozone loss derived using tracer-tracer correlations. The detailed discussion about the location of profiles in Sect. 5 was performed to distinguish between profiles observed within the vortex core and the vortex boundary region. Profiles located within the polar vortex core show largest chemical ozone loss values, as observed by ER-2 during January and February and by HALOE between February and April. Kiruna balloon observations confirm larger local ozone loss values if the observations were taken within the polar vortex core. Profiles that were observed in the vortex boundary region indicate less chemical ozone loss.

During March, Kiruna balloon measurements indicate chemical ozone loss of 24 DU below 380 K. By mid-March 1992, chlorine deactivation had substantially proceeded, dominated by the formation of $ClONO_2$. Nevertheless, balloon-borne measurements (Fig. 11) demonstrate that chlorine was still activated in the altitude range between 345 and 400 K potential temperature, with a maximum active chlorine of ≈1 ppb occurring at ≈380 K. These findings are in agreement with very low HCl mixing ratios observed by HALOE in the polar vortex between January and February below 450 K

ACPD
7, 10097–10129, 2007

(Tilmes et al., 2004). The large amount of ozone loss between 350 and 380 K potential temperature was not found using HALOE observations in March, due to the lack of observations at these altitude levels (not shown). Nevertheless, the comparison of averaged ozone loss profiles of Arctic winters between 1991–1992 and 2002–2003, derived using HALOE observations, shows significantly larger ozone loss values at altitudes below 400 K for the years shortly after the Mt. Pinatubo eruption. Between 400 and 500 K, chemical ozone loss values of 59±20 DU are in agreement with values derived by Rex et al. (2004) for altitudes between 400 and 550 K. Therefore, the influence of enhanced sulfate aerosols between 400–550 K described by Rex et al. (2004) is in agreement with the result found here. Kiruna balloon data show less ozone loss, because of their location within the edge of the polar vortex.

The comparison between ER-2, balloon observations that are not influenced by enhanced aerosol loadings and HALOE observations show a good agreement around and below 400 K. This is the altitude where the uncertainty of HALOE was presumed to be largest. Further, column ozone loss between 400–500 K is in agreement for ER-2 and HALOE observations. Therefore, we conclude the influence of large aerosol loadings on HALOE measurements is small and ozone loss values calculated between February and April are reliable. Chemical ozone loss in winter 1991–1992 is significantly larger than comparable moderately warm winters.

9 Conclusions

In the moderately warm winter 1991–1992 significant chemical ozone loss was found as a result of the enhanced burden of sulfate aerosols in the lower stratosphere. The comparison of different observations corroborates results derived from HALOE satellite observations, especially for altitudes below 400 K. Between 400 and 500 K, 41 DU of chemical ozone loss was estimated between January and April based on ER-2 and HALOE observations. Between 380 and 550 K potential temperature, 74 DU of loss was observed in March and 88 DU during April, based on HALOE observations. For

altitudes below 400 K, large ozone loss of 24 DU was derived based on Kiruna balloon observations, in agreement with activated chlorine of ≈1 ppb occurring at ≈380 K in mid-March 1992.

Acknowledgements. We gratefully acknowledge all members of the HALOE team at NASA Langley for their work in producing a high-quality data set. Thanks are also due to the UK Meteorological Office and the European Centre for Medium-range Weather Forecasts for providing meteorological analyses. In particular, we acknowledge M. Proffitt for providing high quality ozone profiles and M. Loewenstein for providing N_2O profiles taken during the AASE II mission. The University Corporation for Atmospheric Research (UCAR) supported this work.

References

Anderson, J. G., Toohey, D. W., and Brune, W. H.: Free radicals within the Antarctic vortex: The role of CFCs in Antarctic ozone loss, Science, 251, 39–46, 1991. 10098

Bauer, R., Engel, A., Franken, H., Klein, E., Kulessa, G., Schiller, C., and Schmidt, U.: Monitoring the vertical structure of the Arctic polar vortex over northern Scandinavia during EASOE: Regular N_2O profile observations, Geophys. Res. Lett., 21, 1211–1214, 1994. 10103, 10106, 10107

Brandtjen, R., Klüpfel, T., Perner, D., and Knudsen, B.: Airborne measurements during the European Arctic Stratospheric Ozone Experiment: Observations of OClO, Geophys. Res. Lett., 21, 1363–1366, 1994. 10098, 10101

Camy-Peyret, C.: HCl and CH_4 profiles obtained from balloon-borne FTIR during EASOE, Ann. Geophys., 12, 1994. 10104

Cox, R., MacKenzie, A., Müller, R., Peter, T., and Crutzen, P.: Activation of stratospheric chlorine by reactions in liquid sulfuric-acid, Geophys. Res. Lett., 21, 1439–1442, 1994. 10099

Grooß, J.-U. and Müller, R.: The impact of mid-latitude intrusions into the polar vortex on ozone loss estimates, Atmos. Chem. Phys., 3, 395–402, 2003. 10104

Grooß, J.-U., Günther, G., Konopka, P., Müller, R., McKenna, D. S., Stroh, F., Vogel, B., Engel, A., Müller, M., Hoppel, K., Bevilacqua, R., Richard, E., Webster, C. R., Elkins, J. W., Hurst, D. F., Romashkin, P. A., and Baumgardner, D. G.: Simulation of ozone depletion in spring 2000 with the Chemical Lagrangian Model of the Stratosphere (CLaMS), J. Geophys. Res., 107, 8295, doi:10.1029/2001JD000456, 2002. 10111, 10127, 10128

Hervig, M. E., Russell, III, J. M., Larry, L., Daniels, J., Drayson, R. S., and Park, J. H.: Aerosol effects and corrections in the Halogen Occultation Experiment, J. Geophys. Res., 100, 1067–1079, 1995. 10099, 10100, 10103

Lait, L. R.: An alternative form for potential vorticity, J. Atmos. Sci., 51, 1754–1759, 1994. 10105

Lefèvre, F., Brasseur, G. P., Folkins, I., Smith, A. K., and Simon, P.: Chemistry of the 1991–1992 stratospheric winter: Three-dimensional model simulations, J. Geophys. Res., 99, 8183–8195, 1994. 10099

Loewenstein, M., Podolske, J. R., Fahey, D. W., Woodbridge, E. L., Tin, P., Weaver, A., Newman, P. A., Strahan, S. W., Kawa, S. R., Schoeberl, M. R., and Lait, L. R.: New observations of the NOy/N_2O correlation in the lower stratosphere, Geophys. Res. Lett., 20, 2531–2534, 1993. 10103

Manney, G. L., Froidevaux, L., Santee, M. L., Livesey, N. J., Sabutis, J. L., and Waters, J. W.: Variability of ozone loss during Arctic winter (1991 to 2000) estimated from UARS Microwave Limb Sounder measurements, J. Geophys. Res., 108, doi:10.1029/2002JD002634, 2003. 10099, 10104

Michelsen, H. A., Manney, G. L., Gunson, M. R., and Zander, R.: Correlations of stratospheric abundances of NO_y, O_3, N_2O, and CH_4 derived from ATMOS measurements, J. Geophys. Res., 103, 28 347–28 359, 1998. 10102

Müller, R. and Günther, G., A generalized form of Lait's modified potential vorticity, J. Atmos. Sci., 60, 2229–2237, 2003. 10105

Müller, R., Crutzen, P. J., Oelhaf, H., Adrian, G. P., v. Clarmann, T., Wegner, A., Schmidt, U., and Lary, D.: Chlorine chemistry and the potential for ozone depletion in the Arctic stratosphere in the winter of 1991/92, Geophys. Res. Lett., 21, 1427–1430, 1994. 10111, 10112

Müller, R., Schmidt, U., Engel, A., McKenna, D. S., and Proffitt, M. H.: The O_3/N_2O relationship from balloon-borne observations as a measure of Arctic ozone loss in 1991–1992, Q. J. R. Meteorol. Soc., 127, 1389–1412, 2001. 10098, 10099, 10100, 10107, 10109

Müller, R., Tilmes, S., Konopka, P., Grooß, J.-U., and Jost, H.-J.: Impact of mixing and chemical change on ozone-tracer relations in the polar vortex, Atmos. Chem. Phys., 5, 3139–3151, 2005. 10102

Nash, E. R., Newman, P. A., Rosenfield, J. E., and Schoeberl, M. R.: An objective determination of the polar vortex using Ertel's potential vorticity, J. Geophys. Res., 101, 9471–9478, 1996. 10103, 10105, 10106, 10121, 10122

Naujokat, B., Petzold, K., Labitzke, K., Lenschow, R., Rajewski, B., Wiesner, M., and Wohlfart, R.: The stratospheric winter 1991/92, the winter of the European Arctic Stratospheric Ozone Experiment, Beilage zur Berliner Wetterkarte, Freie Universität Berlin, 1992. 10104

Newman, P. A., Lait, L. R., Schoeberl, M. R., Nash, E. R., Kelly, K., Fahey, D. W., Nagatani, R., Toohey, D., Avallone, L., and Anderson, J.: Stratospheric meteorological conditions in the Arctic polar vortex, 1991–1992, Science, 261, 1143–1156, 1993. 10104

Oelhaf, H., v. Clarmann, T., Fischer, H., Friedl-Vallon, F., Fritzsche, C., Linden, A., Piesch, C., Seefeldner, M., and Völker, W.: Stratospheric $ClONO_2$ and HNO_3 profiles inside the Arctic vortex from MIPAS-B limb emission spectra obtained during EASOE, Geophys. Res. Lett., 21, 1263–1266, 1994. 10101, 10104

Plumb, R. A., Waugh, D. W., and Chipperfield, M. P.: The effect of mixing on tracer relationships in the polar vortices, J. Geophys. Res., 105, 10 047–10 062, 2000. 10102

Proffitt, M. H. and McLaughlin, R. J.: Fast-response dual-beam UV absorption ozone photometer suitable for use on stratospheric balloons, Rev. Sci. Instr., 54, 1719–1728, 1983. 10103

Proffitt, M. H., Aikin, K., Margitan, J. J., Loewenstein, M., Podolske, J. R., Weaver, A., Chan, K. R., Fast, H., and Elkins, J. W.: Ozone loss inside the northern polar vortex during the 1991-1992 winter, Science, 261, 1150–1154, 1993. 10098, 10100, 10101

Pyle, J. A., Harris, N. R., Farman, J. C., Arnold, F., Braathen, G., Cox, R. A., Faucaon, P., Jones, R. L., Megie, G., O'Neill, A., Platt, U., Pommereau, J.-P., Schmidt, U., and Stordal, F.: An overview of the EASOE campaign, Geophys. Res. Lett., 21, 1191–1194, 1994. 10098, 10103

Rex, M., von der Gathen, P., Harris, N. R. P., Lucic, D., Knudsen, B. M., Braathen, G. O., Reid, S. J., De Backer, H., Claude, H., Fabian, R., Fast, H., Gil, M., Kyrö, E., Mikkelsen, I. S., Rummukainen, M., Smit, H. G., Stähelin, J., Varotsos, C., and Zaitcev, I.: In situ measurements of stratospheric ozone depletion rates in the Arctic winter 1991/92: A Lagrangian approach, J. Geophys. Res., 103, 5843–5853, 1998. 10098

Rex, M., Salawitch, R. J., von der Gathen, P., Harris, N. R., Chipperfield, M. P., and Naujokat, B.: Arctic ozone loss and climate change, Geophys. Res. Lett., 31, L04116, doi:10.1029/2003GL018844, 2004. 10099, 10100, 10113

Rex, M., Salawitch, R., Deckelmann, H., von der Gathen, P., Harris, N., Chipperfield, M., Naujokat, B., Reimer, E., Allaart, M., Andersen, S., Bevilacqua, R., Braathen, G., Claude, H., Davies, J., Backer, H. D., Dier, H., Dorokov, V., Fast, H., Gerding, M., Godin-Beekmann, S., Hoppel, K., Johnson, B., Kyrö, E., Litynska, Z., Moore, D., Nakane, H., Parrondo, M., Ris-

ley, A., Jr., Skrivankova, P., Stübi, R., Viatte, P., Yushkov, V., and Zerefos, C.: Arctic winter 2005: Implications for stratospheric ozone loss and climate change, Geophys. Res. Lett., 33, L23308, doi:10.1029/2006GL026731, 2006. 10100

Robock, A.: Volcanic eruptions and climate, Rev. Geophys., 38, 191–219, 2001. 10101

Russell, J. M., Gordley, L. L., Park, J. H., Drayson, S. R., Tuck, A. F., Harries, J. E., Cicerone, R. J., Crutzen, P. J., and Frederick, J. E.: The Halogen Occultation Experiment, J. Geophys. Res., 98, 10 777–10 797, 1993. 10099, 10103

Salawitch, R. J., Wofsy, S. C., Gottlieb, E. W., Lait, L. R., Newman, P. A., Schoeberl, M. R., Loewenstein, M., Podolske, J. R., Strahan, S. E., Proffitt, M. H., Webster, C. R., May, R. D., Fahey, D. W., Baumgardner, D., Dye, J., Wilson, J. C., Kelly, K. K., Elkins, J. W., Chan, K. R., and Anderson, J. G.: Chemical loss of ozone in the Arctic polar vortex in the winter of 1991–1992, Science, 261, 1146–1154, 1993. 10098, 10099

Salawitch, R. J., Margitan, J., Sen, B., Toon, G. C., Osterman, G. B., Rex, M., Elkins, J. W., Ray, E. A., Moore, F. L., Hurst, D. F., Romashkin, P. A., Bevilacqua, R. M., Hoppel, K., Richard, E. C., and Bui, T. P.: Chemical loss of ozone during the Arctic winter of 1999–2000: an analysis based on balloon-borne observations, J. Geophys. Res., 107, 8269, doi:10.1029/2001JD000620, 2002. 10102

Schmidt, U., Kulessa, G., Klein, E., Röth, E.-P., Fabian, P., and Borchers, R.: Intercomparison of balloon-borne cryogenic whole air samplers during the MAP/GLOBUS 1983 campaign, Planet Space Sci, 35, 647–656, 1987. 10103

Schmidt, U., Bauer, R., Engel, A., Borchers, R., and Lee, J.: The variation of available chlorine Cl_y in the Arctic polar vortex during EASOE, Geophys. Res. Lett., 21, 1215–1218, 1994. 10100, 10106, 10107, 10111

Simpson, I. J., Blake, D. R., and Rowland, F. S.: Implications of the recent fluctuations in the growth rate of troposheric methane, Geophys. Res. Lett., 29, doi:10.1029/2001GL014521, 2002. 10111

Tabazadeh, A., Drdla, K., Schoeberl, M. R., Hamill, P., and Toon, O. B.: Arctic "ozone hole" in a cold volcanic stratosphere, Proc. Natl. Acad. Sci., 99, 2609–2612, 2002. 10099

Tilmes, S., Müller, R., Grooß, J.-U., and Russell, J. M.: Ozone loss and chlorine activation in the Arctic winters 1991–2003 derived with the tracer-tracer correlations, Atmos. Chem. Phys., 4, 2181–2213, 2004. 10099, 10101, 10102, 10103, 10109, 10110, 10112, 10113

Tilmes, S., Müller, R., Engel, A., Rex, M., and Russell III, J. M.: Chemical ozone loss in the Arctic and Antarctic stratosphere between 1992 and 2005, Geophys. Res. Lett., 33, L20812,

doi:10.1029/2006GL026925, 2006. 10099, 10100, 10104, 10119

Toohey, D. W., Avallone, L. M., Lait, L. R., Newman, P. A., Schoeberl, M. R., Fahey, D. W., Woodbrige, E. L., and Anderson, J. G.: The seasonal evolution of reactive chlorine in the northern hemisphere stratosphere, Science, 261, 1134–1136, 1993. 10098, 10101, 10110, 10111, 10112

von Clarmann, T., Fischer, H., Friedl-Vallon, F., Linden, A., Oelhaf, H., Piesch, C., and Seefeldner, M.: Retrieval of stratospheric O_3, HNO_3 and $ClONO_2$ profiles from 1992 MIPAS-B limb emission spectra: Method, results, and error analysis, J. Geophys. Res., 98, 20 495–20 506, 1993. 10101, 10104

von der Gathen, P., Rex, M., Harris, N. R. P., Lucic, D., Knudsen, B. M., Braathen, G. O., De Backer, H., Fabian, R., Fast, H., Gil, M., Kyrö, E., Mikkelsen, I. S., Rummukainen, M., Stähelin, J., and Varotsos, C.: Observational evidence for chemical ozone depletion over the Arctic in winter 1991–1992, Nature, 375, 131–134, 1995. 10099, 10110

von Hobe, M., Ulanovsky, A., Volk, C. M., Grooß, J.-U., Tilmes, S., Konopka, P., Günther, G., Werner, A., Spelten, N., Shur, G., Yushkov, V., Ravegnani, F., Schiller, C., Müller, R., and Stroh, F.: Severe ozone depletion in the cold Arctic winter 2004-05, Geophys. Res. Lett., 33, L17815, doi:10.1029/2006GL026945, 2006. 10119

Waters, J. W., Froidevaux, L., Read, W. G., Manney, G. L., Elson, L. S., Flower, D. A., Jarnot, R. F., and Harwood, R. S.: Stratospheric ClO and ozone from the Microwave Limb Sounder on the Upper Atmosphere Research Satellite, Nature, 362, 597–602, 1993. 10098, 10101, 10110

Webster, C. R., May, R. D., Trimble, C. A., Chave, R. G., and Kendall, J.: Aircraft laser infrared absorption spectrometer (ALIAS) for in situ atmospheric measurements of HCl, N_2O, CH_4, NO_2, and HNO_3, Appl. Opt., 33, 454–472, 1994. 10103

Wetzel, G., von Clarmann, T., Oelhaf, H., and Fischer, H.: Vertical profiles of N_2O_5 along with CH_4, N_2O, and H_2O in the late arctic winter retrieved from MIPAS-B infrared limb emission measuerements, J. Geophys. Res., 100, doi:10.1029/95JD02344, 1995. 10101, 10104

WMO, Scientific assessment of ozone depletion: 2006, Global Ozone Research and Monitoring Project-Report No. 50, Geneva, Switzerland, 2007. 10099, 10111, 10127

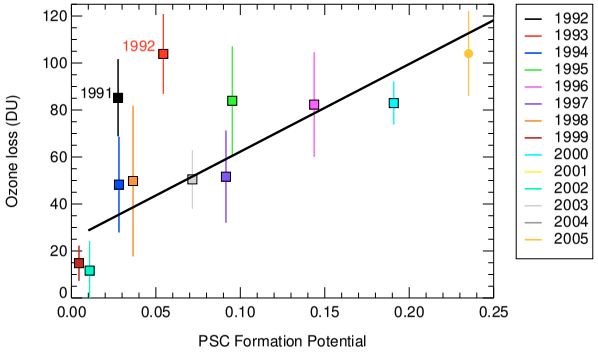

Fig. 1. Relation between the column ozone loss (DU) in March and the PSC formation potential (PFP) for the years 1992 to 2005 between 380–550 K using the tracer-tracer method (colored solid squares), taken from Tilmes et al. (2006) for the Arctic, only. The linear relation for the Arctic (calculated excluding winters 1992 and 1993 that are strongly impacted by the eruption of Mt. Pinatubo) is shown as a black line. Moreover, ozone loss values calculated from the O_3 measurements onboard M55 Geophysica (solid circle) (von Hobe et al., 2006) are shown.

ACPD
7, 10097–10129, 2007

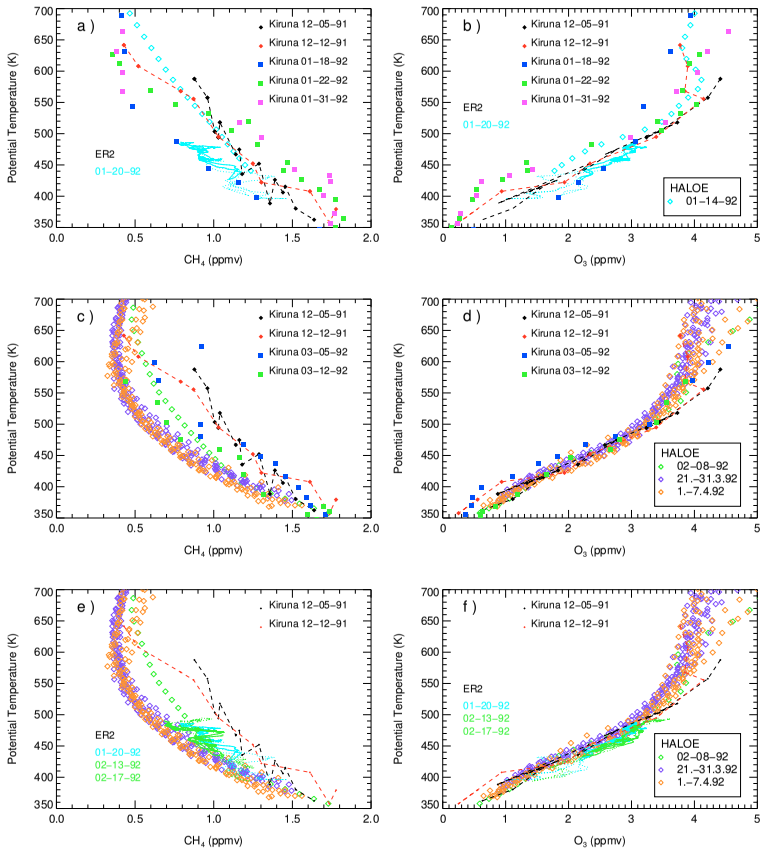

Fig. 2. CH_4 (left column) and O_3 (right column) mixing ratios with respect to potential temperature taken by the HALOE satellite, Kiruna balloons and ER-2 aircraft observations within the vortex core (solid lines) and within the entire vortex (dotted lines), for different periods (see text). Kiruna balloon observations during December (red and black symbols and dashed lines) are shown in each panel as early winter reference profiles.

ACPD
7, 10097–10129, 2007

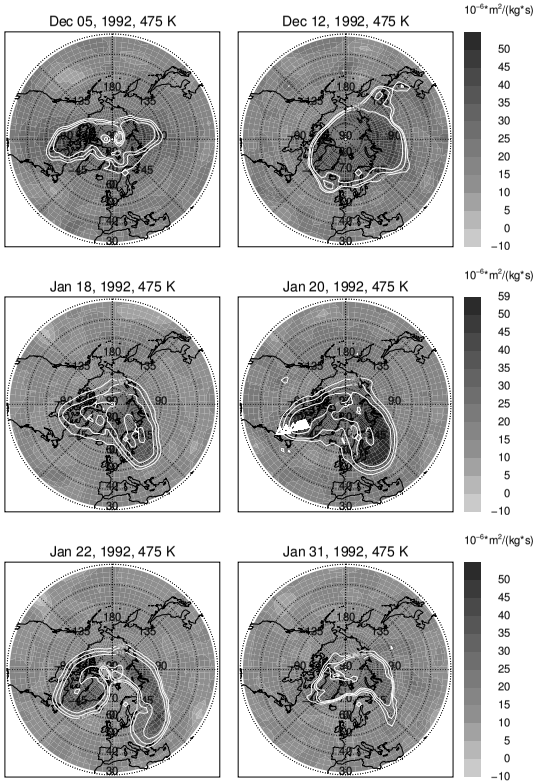

Fig. 3. Potential vorticity derived from MetO analysis on the 475 K potential temperature level valid for 5, 12 December, and 18, 20, 22 and 31 January 1992, 12:00 UTC. White lines indicate the location of the polar vortex core, edge, and outer edge of the vortex as defined by Nash et al. (1996). The location of Kiruna is marked as a white diamond. For the same altitude the location of ER-2 aircraft measurements presented as white triangles for 20 January, only (taken within 8 h at the shown day).

ACPD
7, 10097–10129, 2007

EGU

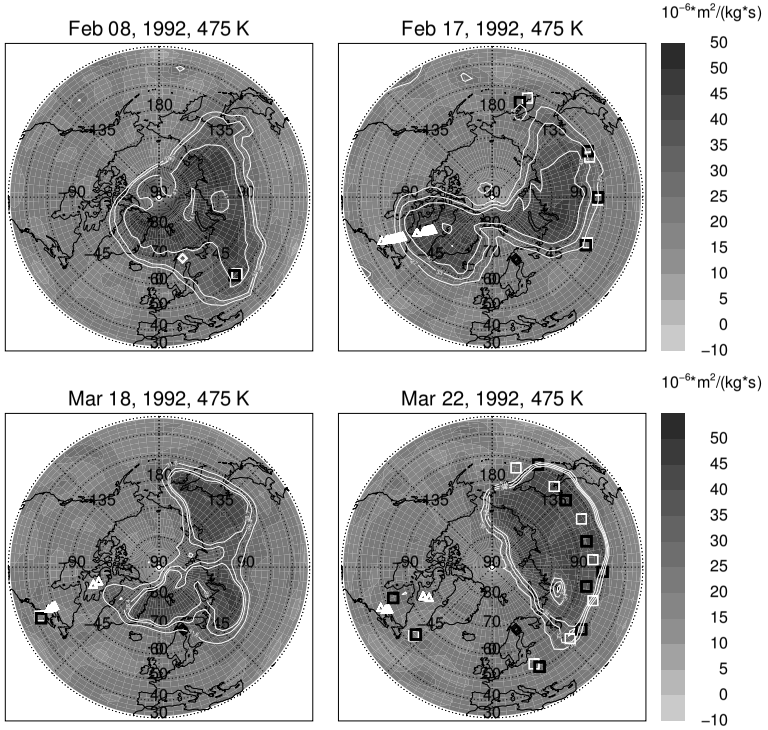

Fig. 4. Potential vorticity derived from MetO analysis on the 475 K potential temperature level valid for 8, 15 February, 18 and 22 March 1992, 12:00 UTC. White lines indicate the location of the polar vortex core, edge, and outer edge of the vortex as defined by Nash et al. (1996). Available HALOE satellite profiles are represented as white squares and ER-2 aircraft measurements are presented as white triangle. The HALOE satellite profiles were repositioned to 12:00 UTC through trajectory calculations, black squares.

ACPD
7, 10097–10129, 2007

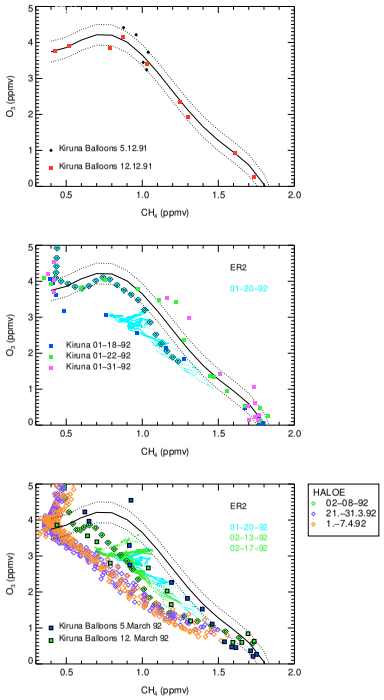

Fig. 5. O_3/CH_4 relations, the early winter reference function was derived using Kiruna balloon data, 5 and 12 December 1991, shown as a black line. Middle panel: O_3/CH_4 relations during January 1992 using ER-2 aircraft measurements within the entire vortex (cyan dotted lines) and within the vortex core (cyan solid lines), Kiruna balloon data (colored squares) and HALOE satellite observations (cyan diamonds) within the polar vortex. Bottom panel: O_3/CH_4 relations between January 1992 and February using ER-2 aircraft measurements within the vortex (cyan and green lines), Kiruna balloon data during March (colored squares) and HALOE satellite observations between February and April (colored diamonds) within the polar vortex. The early winter reference function and its uncertainty is shown in each of the three panels.

ACPD
7, 10097–10129, 2007

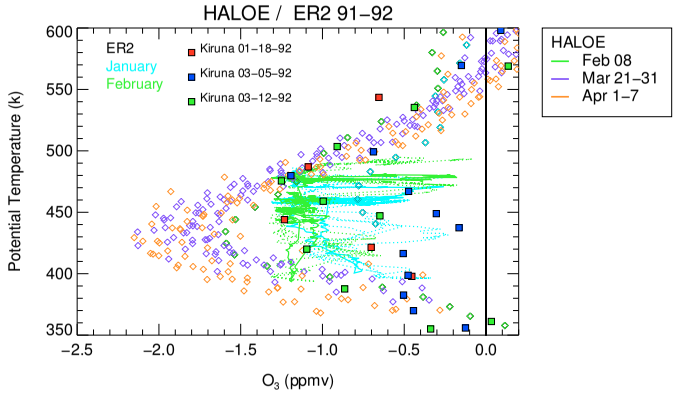

Fig. 6. Ozone loss profiles derived from O_3/CH_4 tracer relations between January und April (see text).

ACPD
7, 10097–10129, 2007

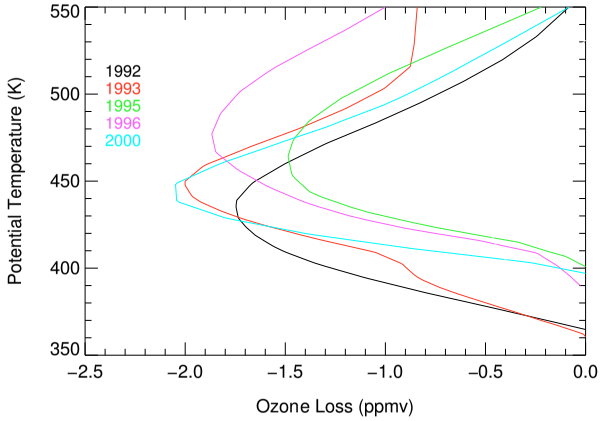

Fig. 7. Averaged ozone loss profiles for March/April for winter 1991–1992, 1992–1993 and cold Arctic winters 1994–1995, 1995–1996 and 1999–2000.

ACPD
7, 10097–10129, 2007

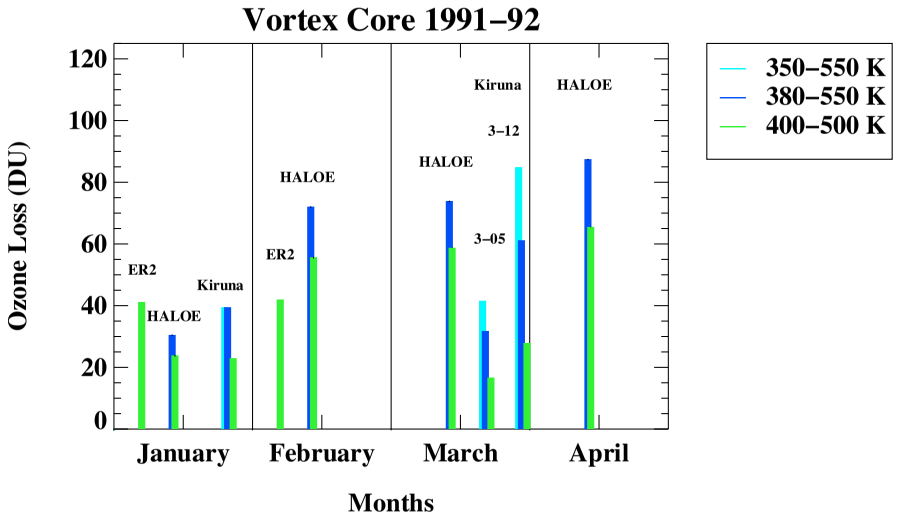

Fig. 8. Accumulated chemical loss in column ozone for different altitude intervals and different months in winter 1991–1992, derived using ER-2 aircraft measurements, HALOE satellite observations, and Kiruna balloon measurements within the vortex core, for different partical columns (see legend).

ACPD
7, 10097–10129, 2007

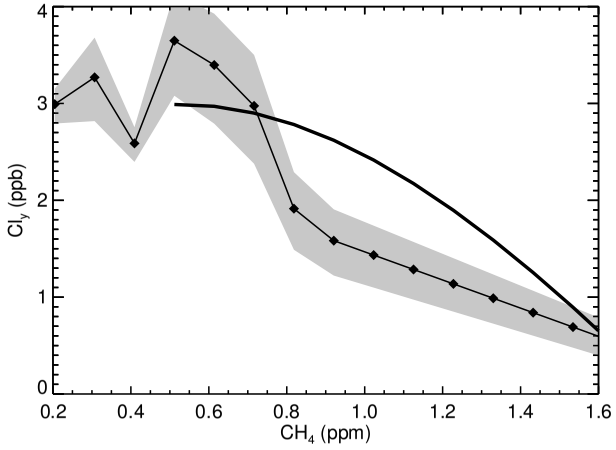

Fig. 9. The sum of $ClONO_2$ (measured by MIPAS-B on 14/15 March 1992) and HCl (measured by LPMA on 14 March 1992) against methane mixing ratios, solid diamonds. The grey scale indicates the combined uncertainty range of $ClONO_2$ and HCl. Also shown is the Cl_y/CH_4 relation from Grooß et al. (2002) (solid black line) where Cl_y has been reduced by 12%, to account for the lower chlorine loading in 1992 than in 2000 (WMO, 2007).

ACPD
7, 10097–10129, 2007

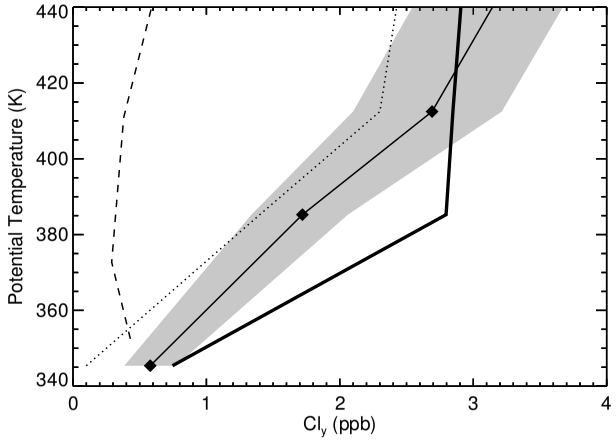

Fig. 10. Similar as in Fig. 9, but here the sum of $ClONO_2$ and HCl mixing ratios (solid diamonds) is shown against potential temperature. The grey scale indicates the combined uncertainty range of $ClONO_2$ and HCl. Solid black line shows the adjusted Cl_y reference from Grooß et al. (2002), using the MIPAS-B methane measurements. Also shown are $ClONO_2$ mixing ratios (from MIPAS-B, dotted line) and HCl (from LPMA, dashed line).

ACPD
7, 10097–10129, 2007

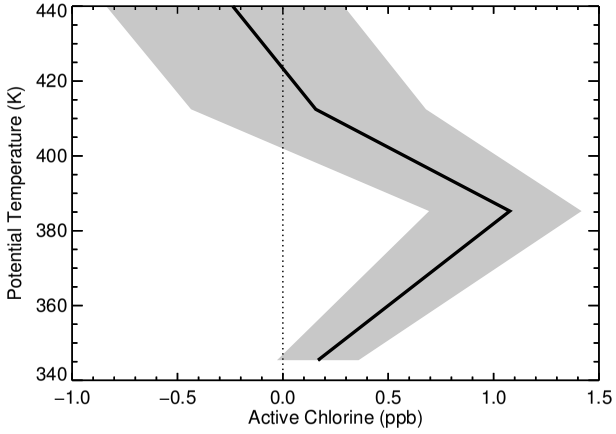

Fig. 11. The vertical profile (against potential temperature) of the mixing ratio of active chlorine on 14 March 1992 in the polar vortex, deduced as the difference between the estimated Cl_y (Fig. 10) and the sum of measured $ClONO_2$ and HCl. The uncertainty (grey range) is derived from the combined uncertainty of $ClONO_2$ and HCl.

ACPD
7, 10097–10129, 2007